Article

Ion Mobility Spectrometry/Mass Spectrometry Snapshots for Assessing the Molecular Compositions of Complex Polymeric Systems

Sarah Trimpin, and David E. Clemmer

More About This Article

Additional resources and features associated with this article are available within the HTML version:

- Supporting Information
- Access to high resolution figures
- Links to articles and content related to this article
- Copyright permission to reproduce figures and/or text from this article

View the Full Text HTML

ACS Publications
High quality. High impact.

Ion Mobility Spectrometry/Mass Spectrometry Snapshots for Assessing the Molecular Compositions of Complex Polymeric Systems

Sarah Trimpin* and David E. Clemmer

Department of Chemistry, Indiana University, Bloomington, Indiana 47405

The synthesis of increasingly complex polymers has created daunting, sometimes insurmountable problems for their chemical analysis. The importance is magnified by outsourcing of production and their use in consumer products, including medical devices and food storage, and therefore requires a new generation of technology for quality assurance. Here, we report capturing subtle differences at the molecular level in complex polymer mixtures nearly instantaneously using a prototype multidimensional ion mobility spectrometry/mass spectrometry spectrometry instrument. Bulk activation/fragmentation strategies reported here provide signatures of structural characteristics that permit effortless recognition of minor differences in blends and copolymers, even as structural isomers and from a quantitative perspective. The data displayed as a pictorial snapshot provide a visual pattern that is sufficiently distinctive that computer-aided pattern recognition can be used to address process control and regulatory issues.

Polymers[1] are ubiquitous in modern society[2] playing key roles in diverse areas from drug delivery to lightweight materials for space flight. These materials are chemically complex mixtures that are prepared from molecular building blocks assembled in various ways to provide two- and three-dimensional (3-D) structures with desirable properties and functions.[3−7] New synthetic methods promise more complexity in which the 3-D shape has functional importance similar to that observed with biopolymers such as proteins.[8] Additionally, the increased use of these materials in association with drugs,[9−11] medical devices,[12] foods,[13] cosmetics,[11] perfumes,[14] nanoparticles,[3,11] and other personal uses, combined with a new era of manufacturer outsourcing, is generating regulatory scrutiny that necessitates detailed knowledge and control of composition.
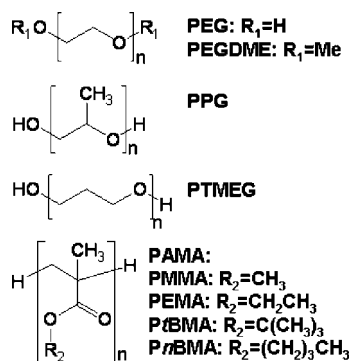
Unfortunately, no analytical method is capable of detailed characterization of complex mixtures of such closely related molecules. Of available techniques, mass spectrometry (MS) is one of the most promising, frequently being employed because of its high sensitivity and mass resolution and, in particular, because of its ability to characterize individual oligomers of a polymer distribution. However, MS methods are limited to measuring only ion intensity and mass-to-charge (m/z) ratios, and information about structure (e.g., differences in polymer sequence or isomers) is inferred indirectly, if at all,[15] through a combination of techniques such as size exclusion chromatography (SEC), liquid adsorption chromatography at critical conditions, light scattering, and nuclear magnetic resonance spectroscopy.[16,17] Additional issues, including solubility and ionization phenomena, further complicate or prevent analysis.[18,19] Strategies that are routinely used for biological materials, such as identification of proteins using peptide fragment ion mass spectral data and sophisticated databases and search algorithms,[20] are currently not applicable for polymer characterization, although initial software for the interpretation of electrospray ionization (ESI)-MS/MS data of synthetic polymers has been described recently.[21] The fundamental importance of relating molecular structure to understanding bulk properties and the need for rapid analysis for quality and regulatory assurance has led to a search for novel means of characterizing polymeric compositions on a molecular level.

* To whom correspondence should be addressed. Current address: Department of Chemistry, Wayne State University, 5101 Cass Ave., Detroit, MI 48202. E-mail: strimpin@chem.wayne.edu. Tel.: (313) 577-9823. Fax: (313) 577-8822.

(1) Staudinger, H. *Ber. Dtsch. Chem. Ges. B* **1920**, *53*, 1073–1085.
(2) Ober, C. K. *Science* **2000**, *288*, 448–449.
(3) Frechet, J. M. J. *Science* **1994**, *263*, 1710–1715.
(4) Stupp, S. I.; LeBonheur, V. V.; Walker, K.; Li, L. S.; Huggins, K. E.; Keser, M.; Amstutz, A. *Science* **1997**, *276*, 384–389.
(5) Friend, R. H.; Gymer, R. W.; Holmes, A. B.; Burroughes, J. H.; Marks, R. N.; Taliani, C.; Bradley, D. D. C.; Dos Santos, D. A.; Bredas, J. L.; Logdlund, M.; Salaneck, W. R. *Nature* **1999**, *397*, 121–128.
(6) Forrest, S. R. *Nature* **2004**, *428*, 911–918.
(7) Hoger, S. *Chem. Eur. J.* **2004**, *10*, 132–1329.
(8) Hawker, C. J.; Wooley, K. L. *Science* **2005**, *309*, 1200–1205.
(9) Discher, D. E.; Eisenberg, A. *Science* **2002**, *297*, 967–973.
(10) Allen, T. M.; Cullis, P. R. *Science* **2004**, *303*, 1818–1822.
(11) Nel, A.; Xia, T.; Madler, L.; Li, N. *Science* **2006**, *311*, 622–627.
(12) Langer, R.; Tirrell, D. A. *Nature* **2004**, *428*, 487–492.
(13) Kaiser, J. *Science* **2007**, *317*, 884–885.
(14) Fieber, W.; Herrmann, A.; Ouali, L.; Velazco, M. I.; Kreutzer, G.; Klok, H.-A.; Ternat, C.; Plummer, C. J. G.; Månson, J.-A. E.; Sommer, H. *Macromolecules* **2007**, *40*, 537–5378.
(15) Trimpin, S.; Eichhorn, P.; Räder, H. J.; Müllen, K. *J. Chromatogr., A* **2001**, *938*, 67–77.
(16) Trimpin, S.; Falkenhagen, J.; Weidner, S. M.; McEwen, C. N. *Anal. Chem.* **2007**, *79*, 7565–7570.
(17) Weidner, S. M.; Trimpin, S. *Anal. Chem.* **2008**, *80*, 4349–4361.
(18) Trimpin, S.; Grimsdale, A. C.; Räder, H. J.; Müllen, K. *Anal. Chem.* **2002**, *74*, 3777–3782.
(19) Trimpin, S.; Keune, S.; Räder, H. J.; Müllen, K. *J. Am. Mass Spectrom.* **2006**, *17*, 661–671.
(20) Cravatt, B. F.; Simon, G. M.; Yates, J. R., III. *Nature* **2007**, *450*, 991–1000.
(21) Thalassinos, K.; Jackson, A. T.; Williams, J. P.; Hilton, G. R.; Slade, S. E.; Scrivens, J. H. *J. Am. Soc. Mass Spectrom.* **2007**, *18*, 1324–1331.

Scheme 1. Primary Structures of Some of the Homopolymers Examined in This Work[a]

[a] The structures include PEGs with different end group functionalities as well as polymers with different repeat units such as poly(propylene glycol) (PPG) and poly(tetramethylene glycol) (PTMEG) and, additionally, several poly(alkyl methacrylate)s (PAMA)s. P*t*BMA and P*n*BMA are structural isomers, thus, differing only in spatial size requirements. Some of these polymeric structures were examined in various different molecular masses, up to ~17.9 kDa in the case of PEG.

Here, we use a home-built instrument that combines ESI with ion mobility spectrometry (IMS) and MS.[22,23] The output of the combined measurements is a multidimensional separation that contains IMS drift time (t_d, in ms) and MS values (m/z) displayed in a nested fashion [$t_d(m/z)$] with a false color image of ion abundances.[24−27] Initial work focused on the principle applicability of this methodology to synthetic poly(ethylene glycol) (PEG) polymers up to 17.9 kDa and includes details concerning instrumentation, data acquisition and charge-state separation, polydispersity, end group, and conformational analysis.[26] Recent work also showed separation of charge states using a commercial IMS−MS system.[28] As shown here, multidimensional IMS−MS methodology provides a detailed view of molecular components in complex mixtures that is based on a combined analysis of the 3-D geometries and masses of polymeric components (Scheme 1) adducted with metal cations in the gas phase.[27]

EXPERIMENTAL SECTION

Materials. Polymer materials (PEGs, PTMEG, PEMA, P*n*-BMA, P*t*BMA) were gifts from Dr. Hofe, Polymer Standard Services (Mainz, Germany); poly(methyl methacrylate) (PMMA) from Dr. Hanton, Air Products (Allentown, PA); and PEGs, PPG, and Jeffamine from Dr. McEwen, DuPont Corporate Center for Analytical Sciences (Wilmington, DE). Structures are provided in Scheme 1. Cesium, lithium, and sodium chloride as well as acetate, respectively, were purchased from Sigma-Aldrich (St. Louis, MO). Acetonitrile and methanol were obtained from Mallinckrodt Baker, Inc. (Philipsburg NJ). Omnisolve water was from EMD Chemicals, Inc. (Gibbstown, NJ).

Instrumentation. The multidimensional ESI-IMS-MS instruments used in this study have previously been described.[22,23] A 2m IMS−MS instrument (Scheme 2) incorporates in addition to the two drift regions (D1 and D2; each ~1 m in length), two ion activation regions (IA1 and IA2) and a robotic nanoflow ion source[29] NanoMate HD autosampling system (NanoMate, Advion BioSciences, Inc., Ithaca, NY) for automated sample introduction. A 3m IMS−MS instrument is similar with the exception of having three consecutive drift tube regions and operating with a conventional ESI source (Supporting Information).

Sample Preparation. Typically, samples were dissolved in 50/50% water/acetonitrile solution at a concentration of 0.25 mg mL^{-1} containing 1 M CsCl (Sigma-Aldrich) and ionized using ESI.

Data Acquisition. Ions are accumulated in the source funnel (F1) and gated through ion gate G1 where they drift through an electric field in a buffer gas (He, ~3 Torr, ~10 V cm^{-1}) promoting mobility separation (Scheme 2). Ions exiting the drift tube through an interface region are focused into the source region of an orthogonal reflectron TOF-mass spectrometer. Drift distributions and mass spectra are recorded as nested drift (flight time) data in units of $t_d(m/z)$, where the value of t_d is given in milliseconds.[24−26] Bulk IMS-activation (a)/fragmentation (f)-IMS (IMS-a/f-IMS) data sets are recorded by energy manipulations at IA1 or IA2. This approach operates selection-free, contrary to other IMS−IMS[22,23,25] or MS/MS methods,[33−35] and allows in a controlled fashion a continuous manipulation of ions causing simultaneous activation (a) (Scheme 2B.2) or, as desired, fragmentation (f) (Scheme 2B.3) of the entire polymer distribution with subsequent separation of these altered ions. IMS-a-IMS strategy (commonly <100 V) manipulates the shape of the ion, evident by additional conformations (Scheme 2B.2) within a specific charge state as well as improved separation of different charge states, through energy-induced structural changes or charge reduction (dissociation of the charge carrier) (Scheme 2B.3,4). In most favorable cases, the activated ion releases cation(s) changing both the charge state and shape. This response to energy adjustment is evident in the displayed image (Scheme 2B.3,4) and enhances the resolution of the drift dimension as compared to the nonactivated experiment (Scheme 2B.1).

Data Analysis. Origin software 6.1 and 7.0 (OriginLab Corp., Northampton, MA) is used for plotting and viewing details of the 2D color-coded images (red most abundant and blue least abundant). Software written in-house was used to extract the total t_d distributions and mass spectra. This software is also used for extracting embedded t_d or m/z data diagonally, vertically, or horizontally by taking slices from the data embedded in the image

(22) Koeniger, S. L.; Merenbloom, S. I.; Valentine, S. J.; Jarrold, M. F.; Udseth, H.; Smith, R.; Clemmer, D. E. *Anal. Chem.* **2006**, *78*, 4161–4174.

(23) Merenbloom, S. I.; Koeniger, S. L.; Valentine, S. J.; Plasencia, M. D.; Clemmer, D. E. *Anal. Chem.* **2006**, *78*, 2802–2809.

(24) Srebalus, C. A.; Li, J. W.; Marshall, W. S.; Clemmer, D. E. *Anal. Chem.* **1999**, *71*, 3918–3927.

(25) Liu, X.; Valentine, S. J.; Plasencia, M. D.; Trimpin, S.; Naylor, S.; Clemmer, D. E. *J. Am. Soc. Mass Spectrom.* **2007**, *18*, 1249–1264.

(26) Trimpin, S.; Plasencia, M. D.; Isailovic, D.; Clemmer, D. E. *Anal. Chem.* **2007**, *79*, 7974–7974.

(27) Isailovic, D.; Trimpin, S.; Kurulugama, R. T.; Clemmer, D. E. Analysis of Homopolymers and Copolymers by Ion Mobility Spectrometry-Mass Spectrometry. 55th ASMS Conference on Mass Spectrometry and Allied Topics, Session Code: MOG pm Slot: 04:30; Indianapolis, IN, June 3−7, 2007.

(28) Bagal, D.; Zhang, H.; Schnier, P. D. *Anal. Chem.* **2008**, *80*, 2408–2418.

(29) Kurulugama, R. T.; Valentine, S. J.; Sowell, R. A.; Clemmer, D. E. *J. Proteomics* **2008**, *21*, 318–331.

(30) Byrd, H. C. M.; McEwen, C. N. *Anal. Chem.* **2000**, *72*, 4568–4576.

(31) Koeniger, S. L.; Merenbloom, S. I.; Clemmer, D. E. *J. Phys. Chem. B* **2006**, *110*, 7017–7021.
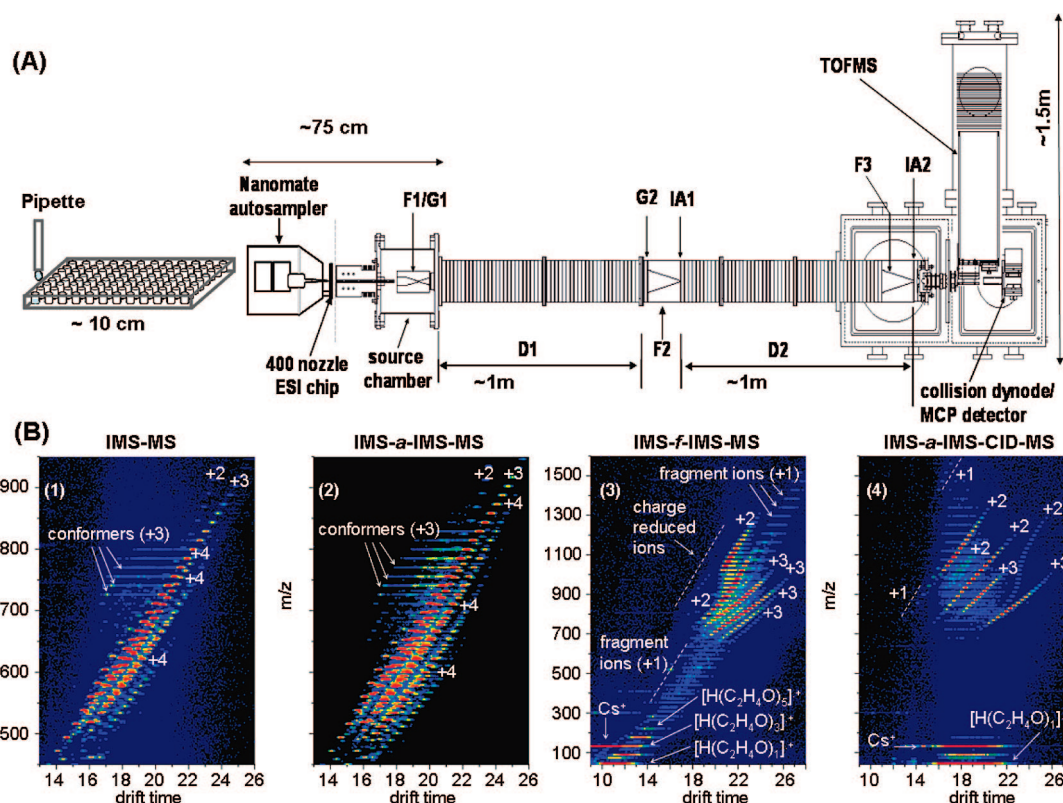
(32) Merenbloom, S. I.; Bohrer, B. C.; Koeniger, S. L.; Clemmer, D. E. *Anal. Chem.* **2007**, *79*, 515–522.

(33) Bogan, M. J.; Agnes, G. R. *J. Am. Mass Spectrom.* **2002**, *13*, 177–186.

(34) Laine, O.; Trimpin, S.; Räder, H. J.; Müllen, K. *Eur. J. Mass Spectrom* **2003**, *9*, 195–201.

(35) Jackson, A. T.; Slade, S. E.; Scrivens, J. H. *Int. J. Mass Spectrom.* **2004**, *238*, 265–277.

Scheme 2. (A) The 2m Drift Tube IMS−MS Instrument Design and Operation[a] and (B) Typical Output for Gas Phase Separated and MS Detected Ions Operated under Different Modes[b]

[a] (1) Operating all drift regions and funnels in transmission mode record the nested IMS−MS datasets. (2–4) The additional energy permits the polymer to attain a different conformation(s), induce dissociation(s) of the cation or covalent bond cleavage(s). Bulk IMS-activation (a)/ fragmentation (f)-IMS data are recorded by operating all drift regions and ion funnels in transmission mode incorporating energy manipulation at IA1. More details to relations between applied voltages and activation (commonly <100 V) vs fragmentation (commonly >140 V) are provided in Figures 4 and 5. Optional elevated voltage at IA2 can be used to induce CID type processes. [b] Images of PEG ∼2000 Da doped with cesium chloride. (1) IMS−MS; (2) IMS-(a)-IMS (activation at IA1); (3) IMS-(f)-IMS (fragmentation at IA1); (4) IMS-(CID)-IMS-MS (fragmentation at IA2).

of any region of interest providing mass spectra or t_d distributions with as little as ∼65 μs in t_d differences. The extracted data are used for structural assignment of polymer(s) such as determining the repeat unit and end groups as well as polymer conformations.

RESULTS AND DISCUSSION

Determination of Low-Abundant High-Mass Components. Long-standing pressing issues in polymer analysis are illustrated by analysis of two different PEG samples, Figure 1. The SEC data (Figure 1A and Supporting Information), which only determine bulk composition, detect a low-abundance high-mass tail extending to ∼12 000 Da on sample 2 (blue), which is not present in sample 1 (green). Matrix-assisted laser desorption/ionization (MALDI) MS (Figure 1B) is able to detect ions from individual oligomers permitting end group analysis, but according to the MALDI-MS data, sample 2 (mass range of ∼2000−4250) differed from sample 1 (mass range of ∼2000−5100) only by a shift in the molecular weight distribution. The high-mass component of sample 2 is not detected. The combination of ESI-IMS-MS is clearly more sensitive to the details of the molecular composition because the separation afforded by the IMS dimension significantly enhances the limited instrumental dynamic range of MS methods.[30] ESI-MS analysis is complicated by the convolution of polymer and charge-state distributions (Supporting Information) and also does not detect the high-mass components.

Figure 1C shows IMS−MS images of the two PEG samples illustrating how visually different these similar samples appear. Polymers adducted with Cs^+ separate into families according to the size, shape, and charge state of the ions. The oligomer mass and end group compositions are determined from any of the charge-state distributions of the IMS−MS data that are observed to extend diagonally across the image as islands. Sample 1 (Figure 1C.1, vendor information M_n = 4250) extends from charge state +2 to +5 (mass range of ∼1100−5400 Da) with the most abundant ions observed for charge state +4 (∼2500−5300 Da). Sample 2 (Figure 2C.2, vendor information M_n = 3400) has charge states ranging from +2 to +11 (mass range of ∼1100−12 200 Da) with the ion intensity peaking at +3 (∼1700−4700 Da).

On the basis of the total IMS−MS distribution, there is a remarkable difference that can be readily observed between samples 1 and 2; at long drift times (50−60 ms), sample 2 exhibits a series of ion families that correspond to polymers in the +6 through +11 charge states. These charge states are entirely absent in sample 1. We conclude that the combination of ESI-IMS-MS is more sensitive to the details of the molecular composition across the entire sample distribution because the instrumental dynamic range is significantly enhanced by the separation afforded by the IMS dimension. In contrast to LC-MALDI approaches for reduction of complexity and enhancement of dynamic range,[15,16]
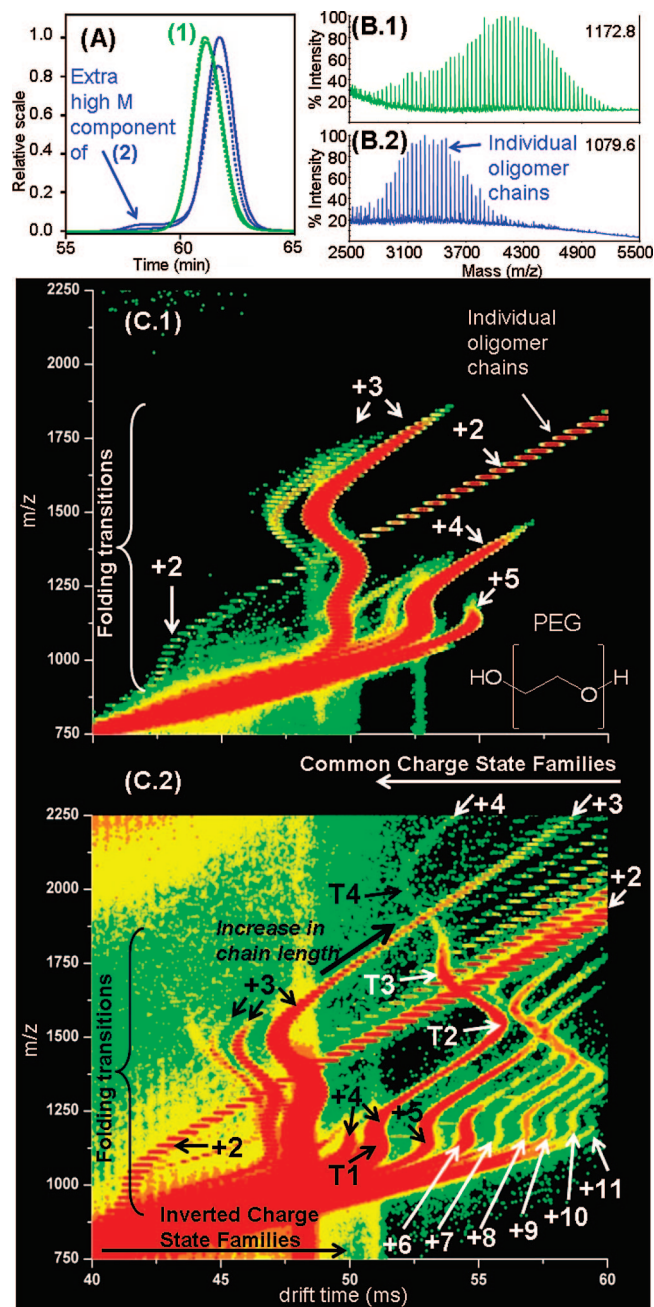
Figure 1. Analyses of two different samples, (1) PEG ~4250 (green) and (2) PEG ~3400 Da (blue), which only vary slightly in molecular composition, utilizing a variety of polymer analyses methods. (A) SEC determines the bulk composition, e.g., polydispersities of ~1.0 were determined for both samples; however, SEC also provides evidence for the high-mass tail of sample 2; dots vs lines indicate different detectors. (B) MALDI-MS of the samples doped with Cs^+ provides singly charged ions of the oligomer chains of similar ion intensity permitting end group analysis; however, MALDI-MS does not permit the detection of the high-mass tail of sample 2. (C) 3-D IMS-MS images (color coding: red most to light blue least abundant) of the samples doped with cesium chloride as charge provider (3m drift tube instrument). Multiple charge-state families are denoted for charge-state families +2 through +5 (sample 1) and +2 through +11 (sample 2), extracted from the mass spectra that are obtained by integration along a diagonal in the $[t_d(m/z)]$ distribution. Details relating to shape, including conformations and folding transitions (T's), are discussed in the text with supporting data provided in Supporting Information. Details of multidimensional IMS−MS instrumentation, data acquisition, and interpretation are provided in the Supporting Information and elsewhere.[23–25] ESI- and MALDI-MS data for samples 1 and 2 are provided in the Supporting Information.

IMS−MS provides a direct measure of all ionized sample components.

Determination of Structural Transitions of Polymeric Materials. Although a quick glance at the IMS−MS data in Figure 1 shows a difference in these polymers beyond the shift in M_n values, there are many characteristics to the shape of these polymeric ions that can be extracted from a more in-depth analysis. This is perhaps best illustrated in Figure 1C.2. An unusual drift inversion occurs at $[t_d(m/z)]$ of about $[40(750)]$ to $[50(900)]$, relative to biological polymers when successively higher charge-state families having extended rather than globular structures drift more slowly in the electric field. In this region, ions appear physically very similar because different charge states vary in t_d by as little as a few tenths of a millisecond.

With increasing polymer chain length (Figure 1C.2), remarkable folding transitions (T's) of these inverted charge-state families occur at a specific polymer m/z (~900−1200) for each charge state, +2 to +11, showing that these multiply charged ions begin to fold producing increasingly globular structures in which the molecular size (as measured by t_d) does not increase with mass. Some even proceed through collapsing transitions (e.g., +4, T2) until a structural density is reached where these polymer ions drift in the IMS dimension similar to proteins (e.g., +3, m/z > 1500; +4, m/z > 2000).[31] The structural differences in shape are corroborated by cross-section analysis (Supporting Information) and are readily visualized by their distinctive sigmoidal contour. For example, $[PEG_{170} + 4Cs]^{4+}$ is significantly smaller (~1000 Å^2) than $[PEG_{120} + 4Cs]^{4+}$ (~1080 Å^2) and about the same size as $[PEG_{80} + 4Cs]^{4+}$ even though the oligomers differ in molecular masses by more than a factor of 2. Images showing these folding transitions and charge-state families are highly specific of polymer size and type.

Conformers of charge state +3 ions were confirmed using an IMS−IMS approach,[23–25,32] which, in analogy to MS/MS,[18,33–35] uses a limited data set in which a specific t_d-selected, energy-activated, ion bundle is examined (Supporting Information). In this region of transitional and conformational evolution, charge-state families pull apart, e.g., as is evident in the large t_d separation of ~2 ms between charge states +4 and +5, permitting the extraction of cleanly separated polymer distributions. The changes in size-to-charge ratios provide signatures for specific types of ions. The enhanced separation in the region of the folding transitions increases the richness of the data set and provides cleanly separated charge states and a nearly instantaneous snapshot for visualizing even small changes in complex polymer systems.

High-Throughput Analysis of Polymeric Materials. The use of chromatographic methods during sample preparation optimization for polymer analysis can be vital to success but places time constraints in particularly in industrial settings.[15,36] Substituting IMS for chromatographic separation promises to reduce the time per analysis; however, IMS separation for synthetic polymer characterization may increase the requirements for proper sample preparation because the gas-phase separation of the polymer chains must increase the analytically useful information and an analytically useful signal is necessary for the mass spectrum. Optimization for IMS−MS may include

(36) Weidner, S. M.; Falkenhagen, J.; Maltsev, S.; Sauerland, V.; Rinken, M. *Rapid Commun. Mass Spectrom.* **2007**, *21*, 2750–2758.
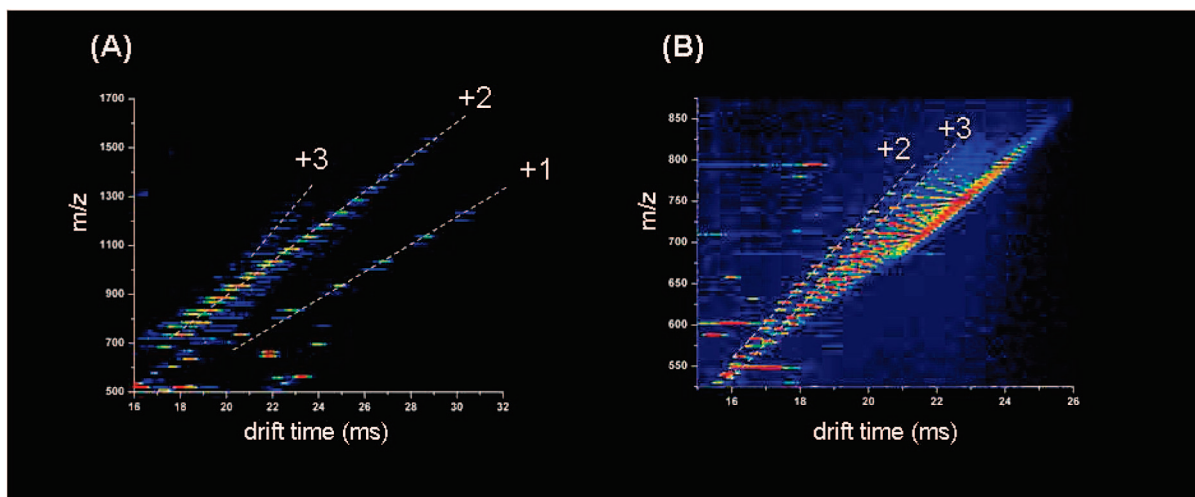
Figure 2. 3-D images attained with the 2m drift tube instrument (Scheme 2) in an automated experiment: (A) PMMA ~6 kDa doped with CsCl using IMS-a-IMS (IA1 = 60 V); (B) PEG ~6 kDa doped with CsCl using IMS−MS (IA1 = 60 V). The unusual drift inversion is only observed for the PEG polymer along with many more charge states (+2 through +10). The charge-state separation of both polymers provides baseline separated ion signals in the extracted mass spectra as described in details for PEG in 26.

variation in cations, analyte concentration, solvents, and even counteranions, as all of these factors effect the analytical outcome of MS polymer characterization.[33−35,37−39] This leads to a matrix of experiments necessary to characterize polymeric materials. These issues are addressed by incorporation of an autosampler for analysis of 96-well sample plates on the 2m IMS−MS instrument (Scheme 2).

In one experiment, 100 samples were continuously acquired in consecutive 5-min acquisitions within ~12 h. Homopolymers (PEG, PEGDME, PPG, PTMEG, PMMA) and blends, in a mass range from ~1 to ~17.9 kDa were examined using different cations (NH_4^+, Li^+, Na^+, Cs^+) and anions (chloride, acetate), all of which provided gas-phase separation and often produced unique features depending on the cation used; representative data sets are provided in Figures 2 and 3 for PMMA, PEG, and PTMEG. The 3-D images of PMMA and PEG, both ~6 kDa, appear drastically different (Figure 2A and B); e.g., drift inversion occurs only in case of PEG, which carries a significant larger number of Cs^+ cations and drifts slower through the drift tube than the PMMA ions.

The influence of the cation on the polymeric structure can be readily visualized; e.g., unique columns are formed when the ammonium cation is used for the ionization of PTMEG (Figure 3C.1), which is not observed for metal cation such as Li^+, Na^+, or Cs^+ (Figure 3C.1 and 2). Apparently, in the case of ionization with NH_4^+, some ions attain very similar shapes as evident in almost identical drift times. With essentially any molar mass of the polymers examined, the cesium cation produces the most efficient gas-phase separation of the individual polymer chains (Figure 3) with the exception of PAMA-based polymers, which provide better signal-to-noise ratios using the sodium cation. Islands of different charge states of PMMA ions are significantly better resolved in the drift dimension than for example PEG ions of about the same mass (6 kDa, Figure 2).

Salt clusters (acetate, chloride) are observed, as can also be seen in Figure 3, particularly with higher molecular weight polymers, and differ for each salt. Other chemical background commonly detected in MS analysis such as solvent-related sig-

nals[40] are also observed. However, the chemical noise does not interfere with the characterization of the polymeric material, except for possible ionization suppression effects addressed in more detail in analysis of polymer blends, because any feature in the 3-D image can be examined exclusively. End group information of all polymeric material (<10 kDa) studied was extractable from each charge-state family.

The analysis of blends and copolymers was sometimes improved by increasing the acquisition time. Nevertheless, clean separation of charge-state families proved challenging, especially on the 2m drift tube instrument. Initial proof-of-principle of a circular drift tube, essentially an unlimited drift tube length, was published recently[41] and may enhance the decongestion of complex polymeric materials even further. However, from a snapshot perspective for control and regulatory purposes, this may not be critical as it is a comparative analysis approach based on visual images. For example, the presence of both PTMEG and PEG (Figure 3) is readily delineated once the image of a homopolymer is established.

Because of the inherent speed of separation of IMS, substituting solvent-free, gas-phase separation for liquid chromatography greatly reduces the time per analysis. Coupled with an autosampler, this approach allows hundreds of images of polymers to be acquired in a high-throughput fashion, indicating applicability to areas in which speed of analysis becomes critical.

Bulk IMS Activation (a)/Fragmentation (f)-MS (IMS-a/f-IMS) Analysis of Polymeric Materials. A bulk IMS-activation (a)/fragmentation (f)-MS (IMS-a/f-IMS) method that allows continuous controlled energy-induced structural changes, cation dissociation, or fragmentation of the polymer backbone, by exposing all ions to elevated voltage without ion selection, is introduced here. This method provides different and reproducible

(37) Chan, K. W. S.; Cook, K. D. *Macromolecules* **1983**, *16*, 1736−1740.
(38) Hanton, S. D. *Chem. Rev.* **2001**, *101*, 527−569.
(39) Montaudo, G.; Samperi, F.; Montaudo, M. S. *Prog. Polym. Sci.* **2006**, *31*, 277−357.
(40) Zhan, D. L.; Fenn, J. B. *Int. J. Mass Spectrom.* **2000**, *194*, 197−208.
(41) Bohrer, B. C.; Merenbloom, S. I.; Koeniger, S. L.; Hilderbrand, A. E.; Clemmer, D. E. *Annu. Rev. Anal. Chem.* **2008**, *1*, 293−327.
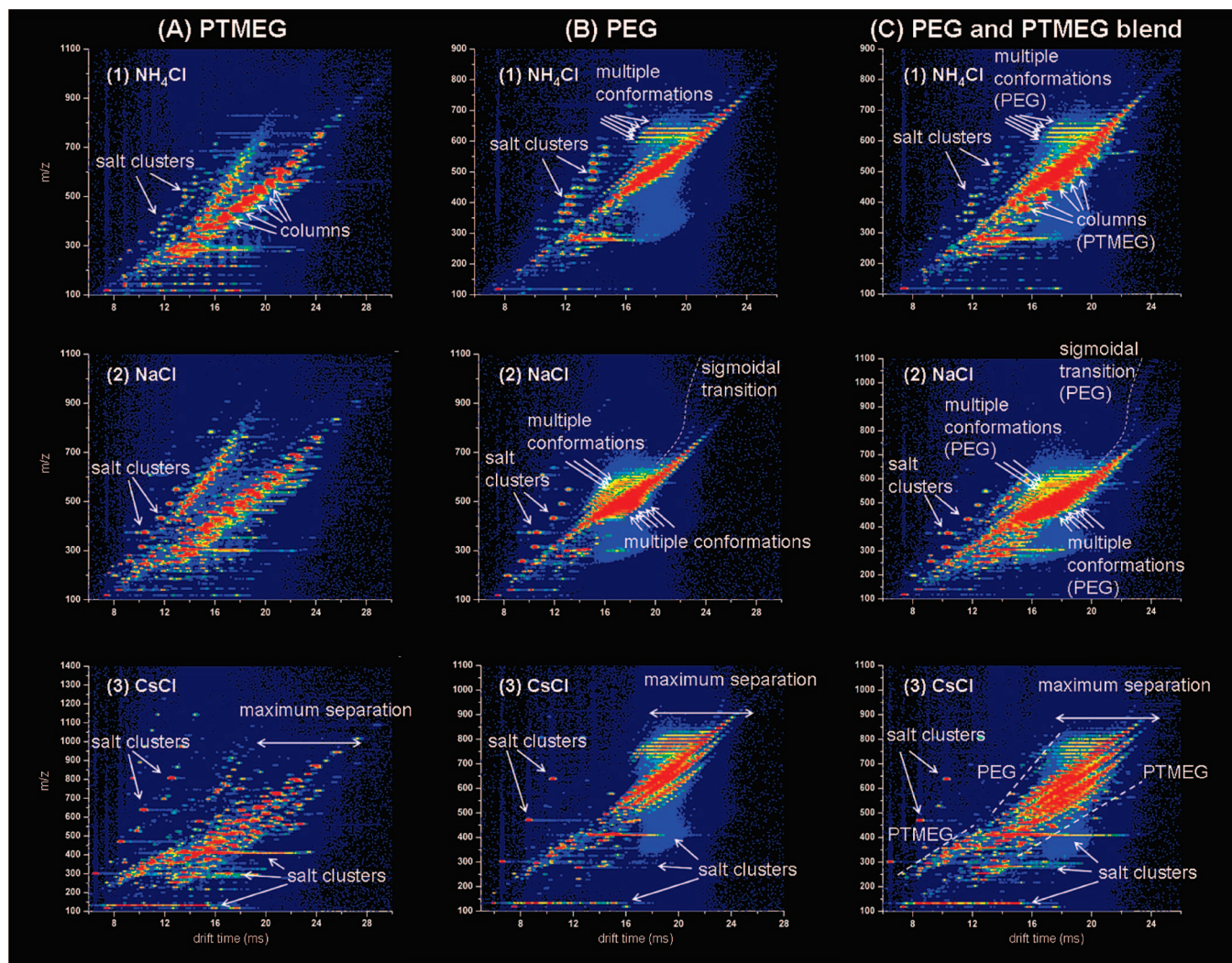
Figure 3. 3-D images attained with the 2m drift tube instrument in an automated experiment: (A) PTMEG; (B) PEG; (C) PTMEG and PEG, doped with (1) NH_4^+, (2) Na^+, and (3) Cs^+. Features for each sample condition provide unique pictorials indicative of a polymer best observed in (C.1) as the "columns" readily identify the presence of PTMEG and the "multiple conformations" the presence of PEG. The presence of the binary blend is not unequivocal under NaCl conditions (C.2). The use of Cs^+ as charge carrier provides a maximum degree of separation and thus decongestion of complexity for both the individual homopolymers and the blend, as even the islands of PEG and PTMEG are partially image-resolved (C.3).

images of the entire activated polymer sample up to ~17.9 kDa and permits end group analysis.

Activation and fragmentation experiments have been performed on a number of polymers in 5-min acquisitions up to 18 kDa. Activated 3-D images (Figures 4 and 5) can be obtained by applying different voltages. While improved separation of the polymeric materials generally occurs below 100 V, charge stripping and fragmentation of the polymer is often induced at higher voltage (>140 V). These different gas-phase processes are readily discerned in the image as can be seen for PEG samples ~2−~17.9 kDa adducted with Cs and Li cations, respectively, applying different degrees of bulk ion activation (0−160 V).

For example, PEG 2 kDa adducted with Cs cation at 0 V shows islands that are almost superimposed (Figure 4.1). At a voltage of 60 V, many conformations are visible and the charge-state islands start to pull apart. At a voltage of 100 V, a maximum degree of separation of the islands is achieved. The onset of dissociation of the charges from the polymer backbone takes place for this system at ~120 V. Fragmentation is observed at ≥140 V.

The dependence of different cations upon energy supply is shown for PEG 17.9 kDa using Cs and Li cations. The polymers adducted with Cs are better resolved in the drift time dimension (Figure 5A and B (1) and (2), respectively). Li cations provide higher fragment ion yields than the Cs cations (Figure 5A and B (3)). Both cations produce identical radical cation fragments of PEG 17.9 kDa that are best described as $[H(OCH_2CH_2)_n]^{+\cdot}$; Cs^+ also produced singly charged ions in the mass range between m/z 600 and 800. The radical cations are identical to the fragment ions produced for PEG ~2000 kDa for which the structure is known to be $HO(CH_2CH_2O)_nH$; both LiCl and CsCl addition to this low molecular weight PEG sample produced $[H(OCH_2CH_2)_n]^{+\cdot}$ utilizing the IMS-f-IMS approach. These IMS-f-IMS results are in accordance with early work on this system utilizing a MS/MS approach of low molecular weight PEG.[42,43] Thus, the PEG 17.9 kDa sample has the structural composition $HO(CH_2CH_2O)_nH$. This assignment has not been possible previ-

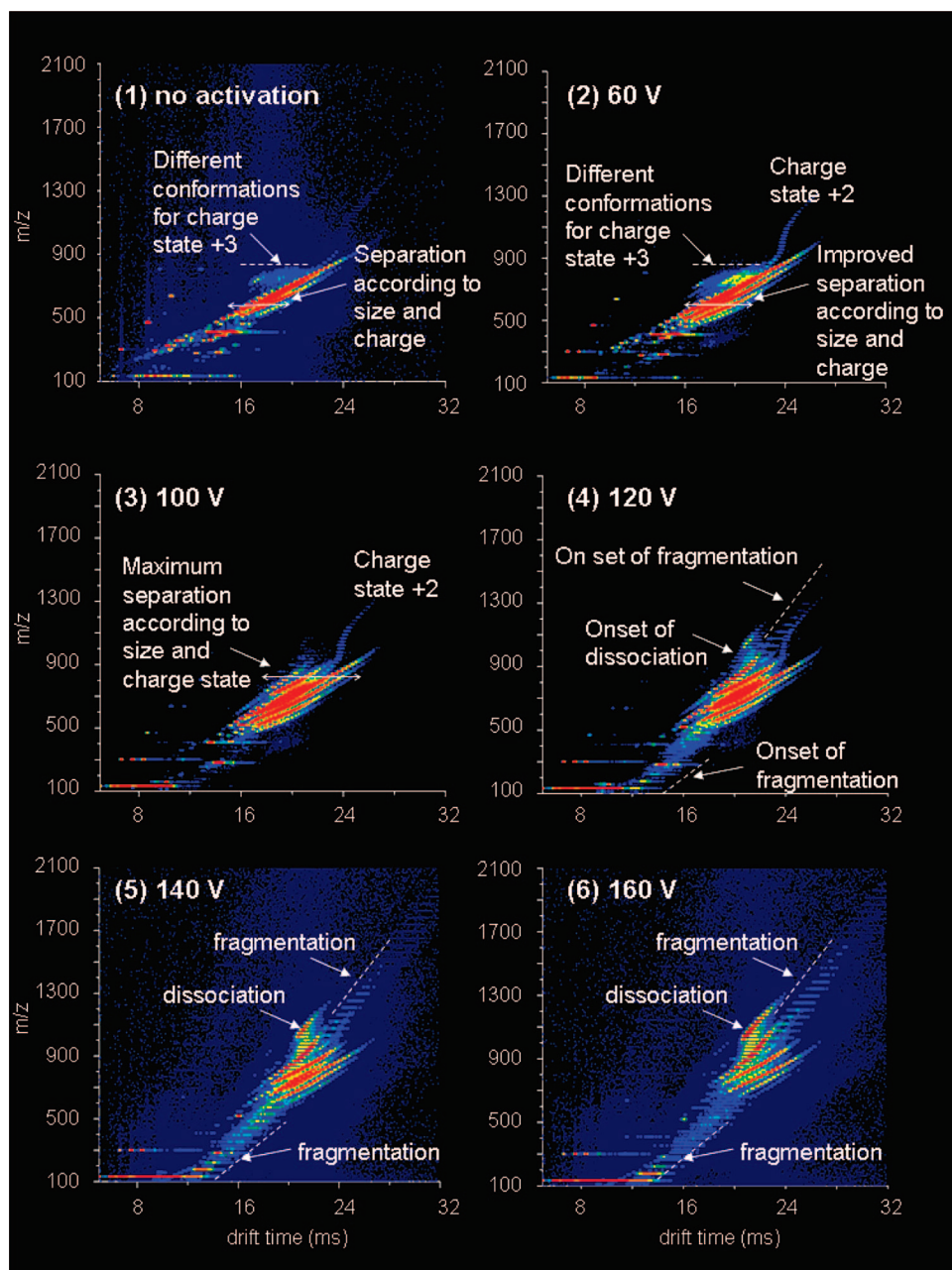(42) Selby, T. L.; Wesdemiotis, C.; Lattimer, R. P. *J. Am. Mass Spectrom.* **1994**, 5, 1081–1092.

Figure 4. Visualization of changes in the 3-D image of PEG ~2 kDa ionized with Cs^+ upon increasing voltages [(1) 0 to (6) 160 V] applied in the middle of the drift tube (here, 2m IMS instrumentation). Voltages of up to 100 V are clean activation experiments (bulk IMS-a-IMS) whereas fragmentation experiments are obtained with ≥140 V (bulk IMS-f-IMS).

ously using IMS−MS due to the combination of the convolution of charge states up to +22 along with the polymer distribution.[26] This methodology, similar to the top-down analysis for protein characterization, clearly extends the accessible mass range for fragment ion analysis beyond other analytical techniques previously employed for polymer analysis.[34]

Bulk fragmentation in the IMS dimension, upon higher energy manipulation of all ions of all charge states, yields high-abundance product ions, because all structures, by differing only in the number of repeat units, produce the same set of fragments. Subsequent separation of these fragment ions in the remainder of the drift tube greatly facilitates interpretation of individual series. Cation dissociation as a response to ion activation enhances the resolving power in 2-D separation but hinders attaining analytically useful fragmentation using a solely MS-based approach.[33–35] This can be seen in the ESI-MS-MS spectra (Supporting Information) of the quadruply Cs^+ adducted PEG ion of m/z-selected 908 in which collisional activation utilizing a commercial high-resolution mass spectrometer results only in loss of Cs^+. These activation experiments also produce additional snapshots that are highly characteristic of the polymer composition and that can be used to further confirm even minor changes in composition. While activated cation dissociation improves the resolving power in 2-D separation, cation removal hinders attaining analytically useful polymer fragment information using a solely MS-based approach.[33–35]

(43) Jackson, T.; Yates, H. T.; Scrivens, J. H.; Critchley, G.; Brown, J.; Green, M. R.; Bateman, R. H. *Rapid Commun. Mass Spectrom.* **1996**, *10*, 1668–1674.
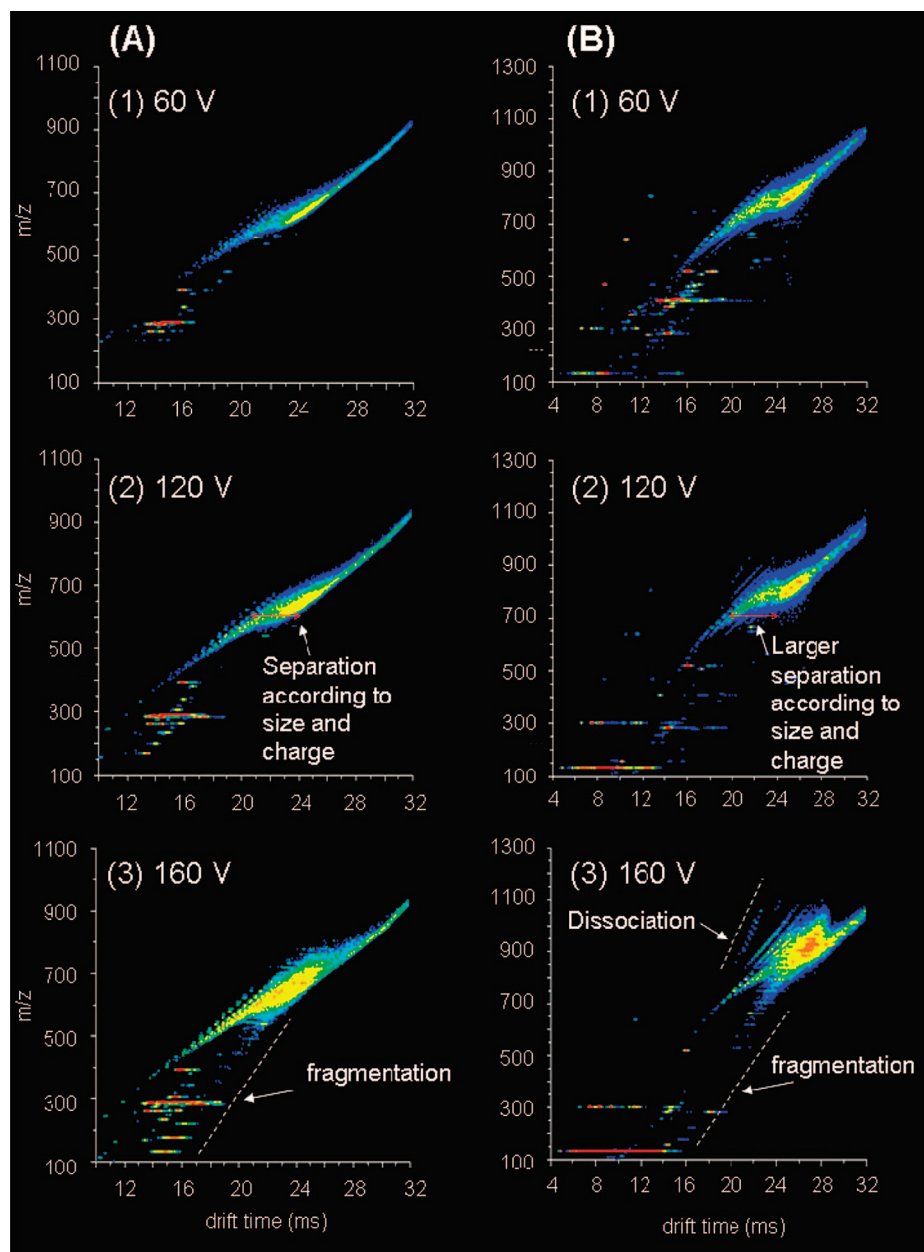
Figure 5. Visualization of changes in the 3-D image of PEG ~17.9 kDa ionized with (A) Li$^+$ and (B) Cs$^+$ upon increasing voltages applied in the middle of the drift tube (here, 2m IMS instrumentation). Cs$^+$ achieves better separation of the charge-state families of the polymer than Li$^+$. Voltages of up to 120 V are clean activation experiments (bulk IMS-a-IMS) whereas fragmentation experiments are obtained with 160 V (bulk IMS-f-IMS). The use of Li$^+$ produces a higher fragment ion yield of PEG 17.9 kDa than Cs$^+$ employing bulk IMS-f-IMS. The dependency of cations used for fragmentation analysis of polymers are described using MALDI and ESI-produced, m/z-selected ions.[33–35]

The bulk fragmentation method is potentially valuable for high-mass polymers for which there is no analytical method available at present for determining end groups. Limitations encountered with MS-based methods are the low abundances of m/z-selected ions and low yields for MS/MS fragment ion analysis of complex mixtures such as polymers. This holds even for multiply charged ions produced by ESI that commonly provide higher fragment ion yields than ions produced by MALDI.[35] Previous studies using postsource decay with MALDI-MS reported producing fragment ions from m/z-selected PMMA ions up to ~10 000 Da but only with significant difficulty, thus providing scant analytical information.[34] With increasing molecular weight of the polymer, slightly better fragment ion yields were observed for the Cs relative to the Li cation.[34] In addition to limited fragmentation, the isobaric

and isomeric compositions of complex polymers also limit the utility of the MS/MS approach for attaining structural information.

Application to the Analysis of Blends. Small changes in the mass of polymer ions, brought about by end group differences, for example, are readily resolved by IMS−MS even when t_d differences are small. As an example, ESI generated ions from a polymer blend (~2000 Da) containing the structures [R$_1$O(CH$_2$CH$_2$O)$_x$R$_1$ + nCs]$^{n+}$, R$_1$ = H [PEG] and R$_1$ = Me [PEGDME] (Figure 6A.1) display distinctive mass spectra for each polymer by extracting m/z values diagonally through the data set: in this case, through the doublets seen in the figure. Even though the t_d separation of the polymer blend with respective charge state +3 is minute, making full use of the two-dimensionality of the IMS–MS dataset by diagonal extraction of the mass spectral data
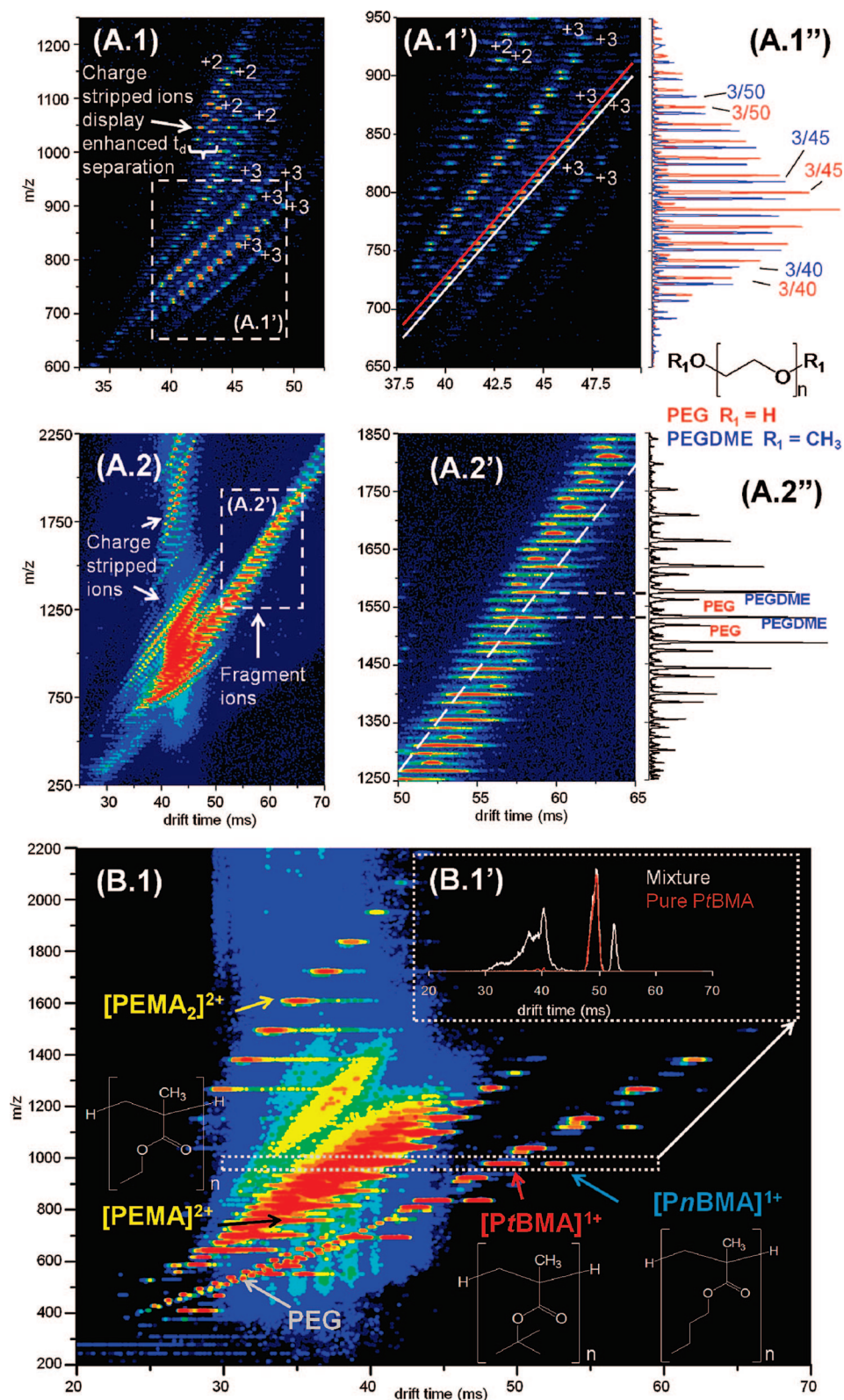
Figure 6. Image analysis of blends of polydisperse macromolecules (here, 3m drift tube instrument). (A) Binary blend of PEG and PEGDME (~2000 Da), differing only by two methyl groups located on the end of each polymer chain (Scheme 1), doped with cesium chloride. Charge-state families for both components are extracted from the mass spectra, including those of the +3 and +2 series; the latter are charge-reduced families with enhanced t_d separation (Δ ~ 1.5 ms). (A.1) Full IMS-a-IMS-MS image (here, 60 V applied at the first activation region). Inset (A.1′) of the most prominent features; dashed lines indicate where mass spectral data were integrated. Slices of one doublet feature, with charge state +3 extracted, showing the two mass spectra overlaid to the right (A.1″) labeled by charge state/number of repeat units (PEG red, PEGDME blue). (A.2) Full IMS-f-IMS-MS image (here, 200 V applied at the first activation region), (A.2′) inset, (A.2″) extracted mass spectrum of one slice. (B) Tertiary blend of PEMA, and the two isomers, P*t*BMA and P*n*BMA (~2000 Da), only differing by the side chains doped with sodium chloride along with low-abundance PEG contamination. (B.1) Full IMS–MS image. Inset (B.1′) of the t_d distribution of the blend against the pure P*t*BMA sample delineating the clean separation of the two isomeric polymers in the tertiary blend. Supporting data to these and studies of other blends are provided in the Supporting Information.
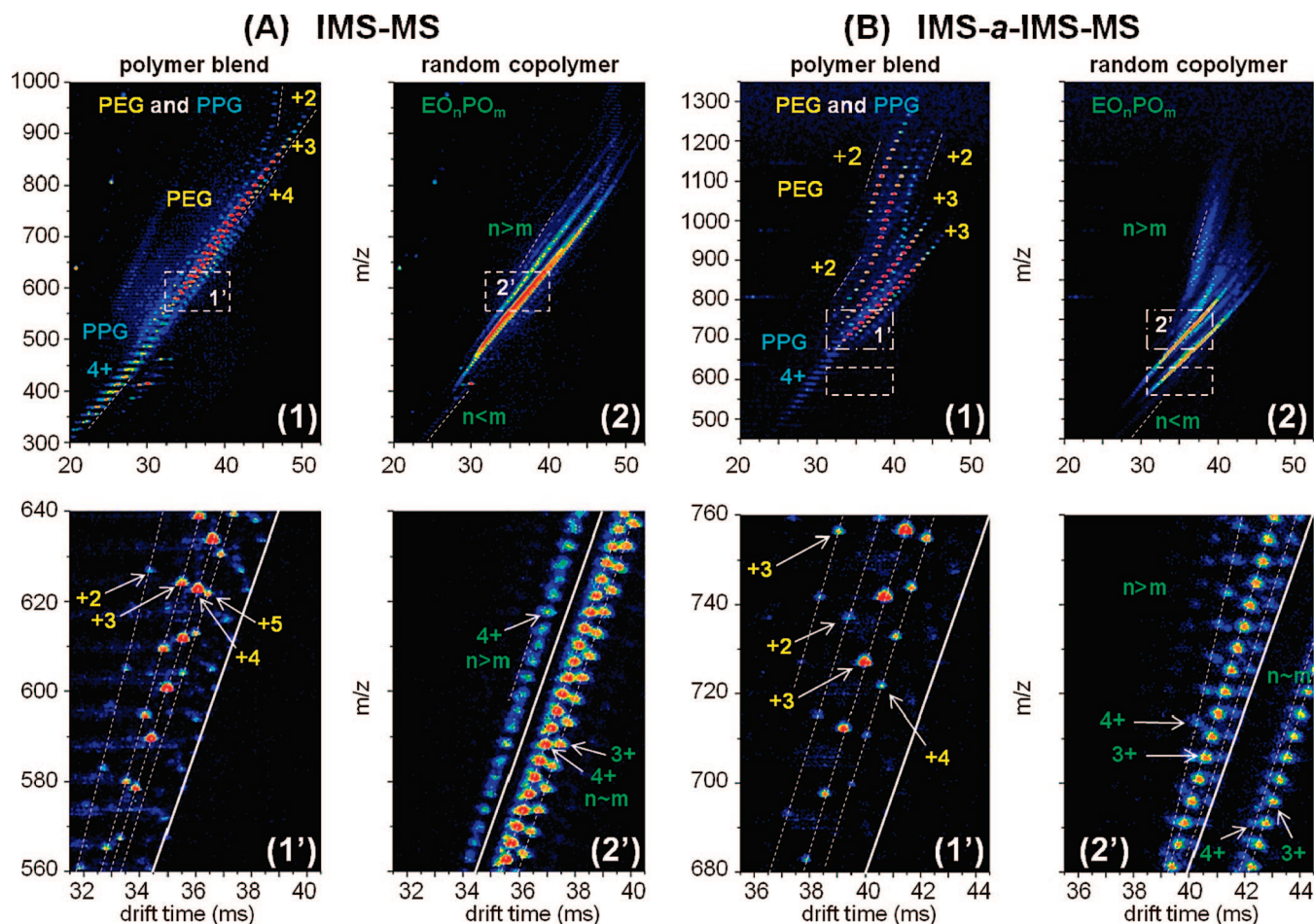
Figure 7. Image analysis (A) IMS−MS and (B) IMS-a-IMS-MS of (1) a blend of PEG (∼2000 Da) and PPG (∼2200 Da) with inset (1′) as well as (2) random copolymer of EO and PO (JEFFamine, ∼2000 Da) doped with cesium chloride with inset (2′). Inset regions (1′, 2′) are indicated with dashed squares in (1, 2); note that the inset regions were taken from areas with the most prominent features and thus differ between (A) and (B). A white line is included to guide the eye for changes within insets of (A) and of (B), respectively. Charge-state families for both samples of different polymeric materials are denoted as extracted from the mass spectra (Supporting Information).

embedded permits the analysis of nearly cleanly separated polymer blends varying only in the end-group functionalities (Figure 6A.1″; red, PEG, blue PEGDME). However, with increasing voltage applied in the center section of the drift tube, cation dissociation (doubly charged in Figure 6A.1) or fragmentation (>140 V; Figure 6A.2), of all ions can be induced simultaneously, which, because of the additional drift region after energy manipulation, provides enhanced m/z and t_d separations. Thus, reduction of charge state(s) by activation introduces changes in m/z and in t_d so that the charge-state families seen in the 3-D image are significantly better resolved, as is apparent in Figure 6A.1. Change stripped ions (+2) display a significantly enhanced separation of $\Delta \sim 1.5$ ms at $m/z \sim 1000$. This manipulation permits the extraction of mass spectra with cleanly separated charge-state families and implies that even more complex mixtures can be separated independent of folding transitions using this methodology.

Bulk activation (Figure 6A.2) combined with the subsequent separation of the altered ions in the reminder of the drift tube has been applied for the analysis of blends. Using the bulk IMS-f-IMS-MS method, high-fragment ion yields, as evident in the extracted mass spectrum (Figure 6A.2″), allowed determination of the end groups of PEG and PEGDME ∼2000 Da without m/z or t_d selection. This method is a notable asset as ions with lower abundance can be accumulated by identical bond cleavage of

different charge states and oligomer lengths while additional unique images are produced at the same time.

Numerous binary and tertiary polymer blends with differences as small as isomeric composition, were examined (Supporting Information). For example, Figure 6B shows a tertiary mixture of three poly(alkyl methacrylates), ethyl (PEMA), *tert*-butyl (P*t*BMA), and *n*-butyl (P*n*-BMA). Spatially larger isomers are always detected at longer drift times; e.g., *n*Bu is more extended than *t*Bu decreasing the ions' mobility through the buffer gas (Figure 6B.1). The successful separation of two isomers within this three-component mixture was confirmed by analyzing the individual isomer samples (Figure 6B.1′). A tertiary blend is difficult to analyze by any analytical technique but even more so when dealing with isomeric compositions. Even using high-resolution MS, the unequivocal characterization of the two isomeric components would not have been possible because of the identical masses. However, the incorporation of the IMS dimension permits the clean separation in time of the two isomers prior to mass detection. Low-abundance PEG contamination is readily characterized as well (Figure 6B.1 and Supporting Information).

Application to the Analysis of Copolymers. The power of the IMS−MS method is perhaps best demonstrated by comparing a blend of polymers made from the same monomer groups (PEG, ∼2000 Da, and PPG, ∼2200 Da) to a random copolymer of ethylene oxide (EO, which can polymerize to PEG) and propylene oxide (PO, which can

polymerize to PPG) (JEFFamine, ~2000 Da), all ionized using ESI with Cs^+ adduction. The ESI mass spectra of the blend and the copolymer are complex and provide little useful information (Supporting Information) because of the numerous oligomers and because each oligomer has multiple charge states. IMS−MS separates both blend and copolymer into charge-state families that are visualized as islands running diagonally across the image (Figure 7), each representing ions with well-defined $[t_d(m/z)]$ coordinates. For example, the one set of islands (Figure 7A.1 and inset A1′) in the blend are determined to be the PEG component with repeat mass 44 Da by inspection of the embedded mass spectral data and by comparison of the 3-D IMS-MS image with those of a PEG standard. The observed m/z differences between the intensity-rich islands range from 22 Da for oligomers carrying two Cs^+ to 8.8 Da for oligomers carrying five Cs^+. Each charge-state distribution allows determination of the repeat unit and end group masses. A further fingerprint of PEG, in addition to the observed drift inversion previously described (Figure 1), is the pronounced effect of energy anipulation on structure and charge states (Figure 7B.1 and inset B.1′).

The PPG component of the blend is defined by a single charge state (+4) with multiple conformers. The conformers are observed as horizontal low-abundant (blue) features in Figure 7A.1 and inset A.1′. The low intensity is the result of the ion signal for each oligomer being spread over a wide t_d range (~1.5 ms). Nevertheless, single charge-state mass spectra free of PEG can be obtained for the PPG oligomers allowing ready determination of repeat unit and end group masses. PPG does not undergo cation dissociation and is only moderately affected by activation, mainly broadening the t_d distribution of each polymeric ion by increasing the number of conformations (Figure 7B.1 and Supporting Information). Although PEG and PPG differ only by a side-chain methyl versus a hydrogen atom, the 3-D patterns are drastically different in the nonactivated (Figure 7A.1) and activated images (Figure 7B.1 and inset B.1′) indicating different energy-release pathways.

The unique 3-D image formed by the copolymer (Figure 7A.2 and inset A.2′) makes this data set visually striking. Similar to the 3-D image of PEG, well-defined, but more closely spaced, diagonal islands are formed (Figure 7A.2′). Two sets of islands are from polymers carrying four Cs^+ and one from polymers with three Cs^+, as determined by the 3.50 and 4.66 spacing along the m/z axis that represent a 14-Da repeating pattern caused by the mass difference of substituting PO (58 Da) for EO (44 Da) along the polymer chain. However, drift inversion is not observed, but during activation (Figure 7B.2 and inset B.2′.1 and inset A.1′), cation dissociation with separation of the charge states is induced, providing a unique image for this copolymer. The mass spectra of the nonactivated image obtained for the more abundant +3 and +4 charge-state families (Supporting Information) shows well-defined baseline-separated signals that produce a Gaussian representation of the polymer distribution in which ions adjacent to one another are of nearly equal intensity. This pattern is representative of a random copolymer in which EO (n) approximately equals PO (m).

On the other hand, the low-abundant charge-state +4 feature (Figure 7A.2′) provides a mass spectrum with a pattern of ion abundances that is indicative of a copolymer in which n and m have different values. The nature of the impurity is unraveled by a combination of characteristics of the 3-D image analysis. The nonactivated image determines the location by the relative $[t_d(m/z)]$ coordination of the impurity that is observed between the pure PEG homopolymer and the randon EO/PO copolymer. Additionally, the activated 3-D image produces intense cation dissociation and drift inversion as previously determined for the PEG homopolymer. These sample characteristics of the copolymer allow us to postulate a low-abundance component that is enriched in the PEG component ($n > m$). Thus, not only is it possible to visually distinguish blends from copolymers, but even compositional differences in copolymers produce images that are readily discerned. Activation further enhances the 2-D separation in a reproducible manner so that subtle differences in polymer composition can be observed in this snapshot image.

CONCLUSION

Blend and copolymer characterization are extremely data- and image-rich, especially applying the IMS-a-IMS-MS strategy, providing signatures of subtle structural characteristics that permit almost instantaneous recognition of sample differences even from a quantitative perspective. Bulk IMS-f-IMS may have powerful implications for polymer analysis similar to top-down approaches for protein analysis. Multidimensional IMS−MS analysis is cost-effective in instrumentation, time of analysis, and the near elimination of consumables associated with liquid separation methods.[15–18] These simple, fast, sensitive, and readily visualized 3-D experiments provide information based upon molecular shape and size, promising to be useful for predicting changes in the physical properties of polymers. Once a snapshot of a blend, copolymer, or other polymer matrix is established, the visual pattern is sufficiently distinctive that, without pursuing detailed analysis of extracting and interpreting embedded mass spectra, it should be possible to address process control and regulatory issues using computer analysis of 3-D images.

SUPPORTING INFORMATION AVAILABLE

Additional information as noted in text. This material is available free of charge via the Internet at http://pubs.acs.org.